Inorg. Chem. **2008**, *47*, 9660−9668

Amidolithium and Amidoaluminum Catalyzed Synthesis of Substituted Guanidines: An Interplay of DFT Modeling and Experiment

Christopher N. Rowley, Tiow-Gan Ong, Jessica Priem, Tom K. Woo,* and Darrin S. Richeson*

Centre for Catalysis Research and Innovation, Department of Chemistry, University of Ottawa, Ontario, Canada, K1N 6N5

Received June 4, 2008

The synthesis of substituted guanidines is of significant interest for their use as versatile ligands and for the synthesis of bioactive molecules. Lithium amides supported by tetramethylethylenediamine have recently been shown to catalyze the guanylation of amines with carbodiimide. In this report, density functional theory (DFT) calculations are used to provide insight into the mechanism of this transformation. The mechanism identified through our calculations is a carbodiimide insertion into the lithium−amide bond to form a lithium guanidinate, followed by a proton transfer from the amine. The proton transfer transition state requires the dissociation of one of the chelating nitrogen centers of the lithium guanidinate, proton abstraction from the amine, and bond formation between the lithium center and the amine nitrogen. On the basis of this mechanism, further calculations predicted that aluminum amides would also function as active catalysts for the guanylation of amines. We confirm this experimentally and report the development of aluminum amides as a new main group catalyst for the guanylation of a range of electron-poor amines with carbodiimide.

Introduction

The guanidine moiety serves as an essential constituent for a number of biologically important molecules.[1] Consequently, there is significant interest in methods to synthesize substituted guanidines, with a typical route being the reaction of an amine with an electrophilic guanylating agent.[2] Guanidines also exhibit flexibility in metal binding modes and have therefore been widely employed in coordination chemistry. Guanidines can coordinate to a metal in a variety of modes, such as a neutral two-electron-donor or a monodentate anionic ligand; however, the bidentate chelating guanidinate ligand has garnered the most interest.[3] This coordination mode provides a stable anionic or dianionic chelating ligand with alkyl substituents that can be modified to adjust the steric, electronic, or thermal properties of the complex. Examples of the guanidinate ligand serving as a support ligand are found in main group,[4−10] transition

* Authors to whom correspondence should be adressed. E-mail: twoo@uottawa.ca (T.K.W.) and darrin@uottawa.ca (D.S.R.).

(1) (a) Mori, A.; Cohen, B. D.; Lowenthal, A. *Guanidines: Historical, Biological, Biochemical and Clinical Aspects of the Naturally Occurring Guanidino Compounds*; Plenum Press: New York, 1985; p 479. (b) Mori, A.; Cohen, B. D.; Koide, H. *Guandines 2: Further Explorations of the Biological and Clinical Significance of Guanidino Compounds*; Plenum Press: New York, 1989; p 365.

(2) (a) Manimala, J. C.; Anslyn, E. V. *Eur. J. Org. Chem.* **2002**, *23*, 3909–3922. (b) Katritzky, A. R.; Rogovoy, B. V. *ARKIVOC* **2005**, 49–87. (c) Schow, S. In *Encyclopedia of Reagents for Organic Synthesis*; Paquette, L. A., Ed.; Wiley: Sussex, U.K., 1995; pp 1408−1410. (d) Ramsden, P. D.; Batey, R. A. *J. Org. Chem.* **2003**, *68*, 2300–2309. (e) Moroni, M.; Koksch, B.; Osipov, S. N.; Crucianelli, M.; Frigerio, M.; Bravo, P.; Burger, K. *J. Org. Chem.* **2001**, *66*, 130–133. (f) Yu, Y.; Ostresh, J. M.; Houghten, R. A. *J. Org. Chem.* **2002**, *67*, 3138–3141. (g) Linton, B. R.; Carr, A. J.; Orner, B. P.; Hamilton, A. D. *J. Org. Chem.* **2000**, *65*, 1566–1568. (h) Tamaki, M.; Han, G.; Hruby, V. J. *J. Org. Chem.* **2001**, *66*, 1038–1042. (i) Ghosh, A. L.; Hol, W. K.; Fan, E. *J. Org. Chem.* **2001**, *66*, 2161–2164. (j) Wu, Y.-Q.; Hamilton, S. K.; Wilkinson, D. E.; Hamilton, G. S. *J. Org. Chem.* **2002**, *67*, 7553–7556. (k) Musiol, H.-J.; Moroder, L. *Org. Lett.* **2001**, *3*, 3859–3861. (l) Katrizky, A. R.; Rogovoy, B. V.; Chassaing, C.; Vvedensky, V *J. Org. Chem.* **2000**, *65*, 8080–8082.

(3) (a) Bailey, P. J.; Pace, S. *Coord. Chem. Rev.* **2001**, *214*, 91–141. (b) Coles, M. P. *Dalton Trans.* **2006**, *8*, 985–1001.

(4) Coles, M. P.; Swenson, D. C.; Jordan, R. F.; Young, V. G., Jr. *Organometallics* **1997**, *16* (24), 5183–5194.

(5) (a) Aeilts, S. L.; Coles, M. P.; Swenson, D. C.; Jordan, R. F.; Young, V. G., Jr. *Organometallics* **1998**, *17* (15), 3265–3270. (b) Hitchcock, P. B.; Lappert, M. F.; Merle, P. G. *Dalton Trans.* **2007**, *5*, 585–594.

(6) Chang, C.-C.; Hsiung, C.-S.; Su, H.-L.; Srinivas, B.; Chiang, M. Y.; Lee, G.-H.; Wang, Y. *Organometallics* **1998**, *17* (8), 1595–1601.

(7) Rowley, C. N.; DiLabio, G. A.; Barry, S. T. *Inorg. Chem.* **2005**, *44* (6), 1983–1991.

(8) Kenney, A. P.; Yap, G. P. A.; Richeson, D. S.; Barry, S. T. *Inorg. Chem.* **2005**, *44* (8), 2926–2933.

(9) Mansfield, N. E.; Coles, M. P.; Hitchcock, P. B. *Dalton Trans.* **2005**, *17*, 2833–2841.

(10) Hill, N. J.; Moore, J. A.; Findlater, M.; Cowley, A. H. *Chem. Commun.* **2005**, *43*, 5462–5464.

10.1021/ic801028m CCC: $40.75
Published on Web 09/24/2008

Scheme 1. The Guanylation of an Amine with Carbodiimide

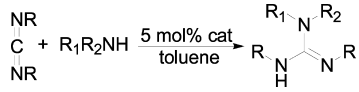

metal,[11] and lanthanide chemistry.[12] Simple and efficient methods to synthesize guanidines will allow for the further advancement of guanidine chemistry in biological applications, as well as the expanded development of metal guanidinate complexes and their uses in catalysis.

A straightforward and atom economical route to guanidine is the guanylation of an amine through its addition to a carbodiimide (Scheme 1). This reaction proceeds directly for nucleophilic amines; however, the guanylation of electron-deficient amines, such as aniline, requires a catalyst. Ti- and V-imido complexes have been found to be effective in this regard.[13,14] These catalysts appear to proceed through the addition of carbodiimide across the metal imido bond, followed by a proton transfer from the amine to this cycloadduct, which releases guanidine and regenerates the reactive metal imido bond. This catalyst pathway is limited to primary amines, and reported examples require elevated temperatures (>100 °C) for the reaction to proceed. Although these catalysts are efficient, their required synthesis can be time-consuming and costly.

Very recently, a half-sandwich yttrium amide complex has been used for the guanylation of secondary amines.[15] This catalyst differs from the Ti- and V-imido catalysts in that the proposed mechanism is the insertion of carbodiimide into a metal amide bond to form a guanidinate ligand (Scheme 2). The resultant guanidinate complex then undergoes a proton transfer with the amine to release the guanidine and regenerate the amido complex. Similarly, a half-sandwich titanacarborane complex has been found to have high guanylation activity, presumably through the same mechanism.[16]

The use of inexpensive, nontoxic alkali,[17] alkali earth,[18] and main group elements[19−21] in the place of transition metals in catalysis is a rapidly developing field. Recently, it

Scheme 2. General Catalytic Cycle for the Guanylation of Amines through the Carbodiimide Insertion—Proton Transfer Mechanism

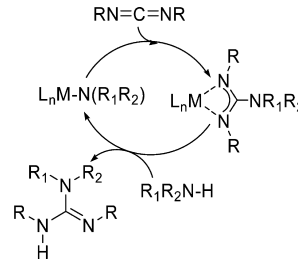

was found that tetramethylethylenediamine (TMEDA)-supported lithium amides[22] are catalysts for the guanylation of electron-deficient amines, operating efficiently under mild reaction conditions.[23] Interestingly, the addition of TMEDA, presumably through modulation of the lithium coordination sphere, increased the reactivity of this catalyst system. While this report included a suggested mechanism for the transformation, a detailed mechanistic understanding would help to explore the generality of the reaction, expand on the range of substrates, and aid in the development of new catalysts/cocatalysts. To the best of our knowledge, the mechanism of guanylation of amines with carbodiimide catalyzed by Li amides or any other catalyst has not been previously examined in detail. In this contribution, we present a density functional theory (DFT) study on the recently demonstrated lithium amide catalyzed guanylation of electron-deficient amines with carbodiimide. This computational study indicated that an analogous catalytic cycle should be available for aluminum amido species, which was corroborated with further calculations. Herein, we also report the computationally motivated development of Al amido complexes as effective main group catalysts for the guanylation of electron-deficient amines with carbodiimide.

Results and Discussion

The Mechanism of Lithium Amide Catalyzed Guanylation. We have modeled the catalytic cycle of the lithium amide/TMEDA catalyzed guanylation of a representative electron-deficient amine, aniline, with diisopropyl carbodiimide.

(11) (a) Tin, M. K. T.; Yap, G. P. A.; Richeson, D. S. *Inorg. Chem.* **1998**, *37* (26), 6728–6730. (b) Bailey, P. J.; Grant, K. J.; Mitchell, L. A.; Pace, S.; Parkin, A.; Parsons, S. *Dalton Trans.* **2000**, (12), 1887–1891. (c) Mullins, S. M.; Duncan, A. P.; Bergman, R. G.; Arnold, J. *Inorg. Chem.* **2001**, *40* (27), 6952–6963. (d) Foley, S. R.; Yap, G. P. A.; Richeson, D. S. *Inorg. Chem.* **2002**, *41* (16), 4149–4157. (e) Baunemann, A.; Winter, M.; Csapek, K.; Gemel, C.; Fischer, R. A. *Eur. J. Inorg. Chem.* **2006**, *22*, 4665–4672. (f) Zhang, W.-X.; Nishiura, M.; Hou, Z. *Chem.—Eur. J.* **2007**, *13* (14), 4037–4051.

(12) (a) Giesbrecht, G. R.; Whitener, G. D.; Arnold, J. *J. Chem. Soc., Dalton Trans.* **2001**, (6), 923–927. (b) Zhang, J.; Cai, R.; Weng, L.; Zhou, X. *J. Organomet. Chem.* **2003**, *672* (1−2), 94–99. (c) Luo, Y.; Yao, Y.; Shen, Q.; Yu, K.; Weng, L. *Eur. J. Inorg. Chem.* **2003**, *2*, 318–323. (d) Chen, J.-L.; Yao, Y.-M.; Luo, Y.-J.; Zhou, L.-Y.; Yong, Z.; Qi, S. *J. Organomet. Chem.* **2004**, *689* (6), 1019–1024. (e) Zhou, S.; Wang, S.; Yang, G.; Li, Q.; Zhang, L.; Yao, Z.; Zhou, Z.; Song, H.-b. *Organometallics* **2007**, *26* (15), 3755–3761. (f) Zhang, L.; Nishiura, M.; Yuki, M.; Luo, Y.; Hou, Z. *Angew. Chem., Int. Ed.* **2008**, *47* (14), 2642–2645.

(13) Ong, T.-G.; Yap, G. P. A.; Richeson, D. S. *Chem. Commun.* **2003**, (20), 2612–2613.

(14) Ong, T.-G.; Yap, G. P. A.; Richeson, D. S. *J. Am. Chem. Soc.* **2003**, *125* (27), 8100–8101.

(15) Zhang, W.-X.; Nishiura, M.; Hou, Z. *Synlett* **2006**, (8), 1213–1216.

(16) Shen, H.; Chan, H.-S.; Xie, Z. *Organometallics* **2006**, *25* (23), 5515–5517.

(17) (a) Boesveld, W. M.; Hitchcock, P. B.; Lappert, M. F. *J. Chem. Soc., Perkin Trans. 1* **2001**, *9*, 1103–1108. (b) Knapp, C.; Lork, E.; Watson, P. G.; Mews, R. *Inorg. Chem.* **2002**, *41* (8), 2014–2025. (c) Zhang, Y.; Reeder, E. K.; Keaton, R. J.; Sita, L. R. *Organometallics* **2004**, *23* (14), 3512–3520. (d) Zhao, P.; Lucht, B. L.; Kenkre, S. L.; Collum, D. B. *J. Org. Chem.* **2004**, *69* (2), 242–249. (e) Harada, T.; Muramatsu, K.; Fujiwara, T.; Kataoka, H.; Oku, A. *Org. Lett.* **2005**, *7* (5), 779–781.

(18) (a) Crimmin, M. R.; Casely, I. J.; Hill, M. S. *J. Am. Chem. Soc.* **2005**, *127* (7), 2042–2043. (b) Harder, S.; Feil, F.; Knoll, K. *Angew. Chem., Int. Ed.* **2001**, *40* (22), 4261–4264. (c) Chisholm, M. H.; Gallucci, J. C.; Phomphrai, K. *Inorg. Chem.* **2004**, *43* (21), 6717–6725.

(19) (a) Susumu, S. Aluminum in Organic Synthesis. In *Main Group Metals in Organic Synthesis*; Wiley-VCH: Weinheim, Germany, 2004; Vol. *1*, pp 189−306. (b) Preston, A. C.; Gregory, C. W. T. J.; Douglas, W. S. *Angew. Chem.* **2007**, *119* (42), 8196–8199.

(20) Dornan, P.; Rowley, C. N.; Priem, J.; Barry, S. T.; Burchell, T. J.; Woo, T. K.; Richeson, D. S. *Chem. Commun.* **2008**, 3645–3647.

(21) (a) Hoerter, J. M.; Otte, K. M.; Gellman, S. H.; Stahl, S. S. *J. Am. Chem. Soc.* **2006**, *128* (15), 5177–5183. (b) Hoerter, J. M.; Otte, K. M.; Gellman, S. H.; Cui, Q.; Stahl, S. S. *J. Am. Chem. Soc.* **2008**, *128* (15), 6.

(22) Collum, D. B. *Acc. Chem. Res.* **1992**, *25* (10), 448–54.

(23) Ong, T.-G.; O'Brien, J. S.; Korobkov, I.; Richeson, D. S. *Organometallics* **2006**, *25* (20), 4728–4730.

Scheme 3. Catalytic Cycle for Guanylation of Aniline with Carbodiimide with a TMEDA Supported Lithium Catalyst

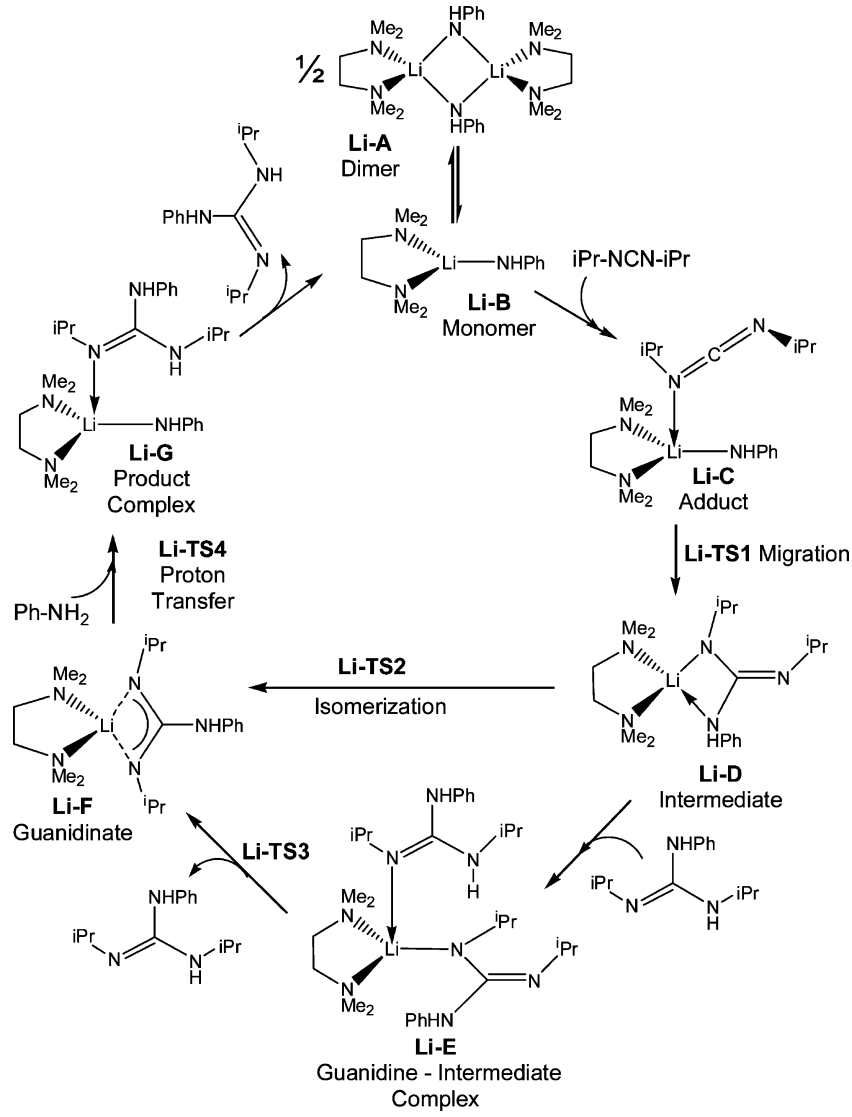

Our proposed reaction mechanism is shown in Scheme 3. Here, we have adopted the following convention for labeling of the stationary points that have been optimized computationally. Minimum-energy structures are labeled "**Li−X**", where **X** is an alphabetic character ranging from **A** to **G**. Transition state structures are designated "**Li−TS#**" where the number sign corresponds to a numeric character assigned sequentially according to discussion in the text. The "**Li−**" prefix is used to distinguish between an analogous mechanism involving an Al catalyst to be discussed in a later section.

The TMEDA coordinated lithium anilide, **Li−B**, as shown in Scheme 3 was used as the putative active catalyst. In order to achieve electronic and steric saturation, this species would likely exist in equilibrium with its dimer species **Li−A**, which is calculated to be 11.1 kcal mol^{-1} more stable than the monomer.

Carbodiimide Insertion. Upon formation of the monomer, the first step of the proposed catalytic cycle involves the insertion of carbodiimide into the Li−NHPh bond. Although the insertion of carbodiimide into lithium amide bonds has been used extensively in synthesis,[9,23−25] no computational study on this topic has been reported. On the other hand, the insertion of carbodiimide into aluminum amide and alkyl bonds has been extensively studied both experimentally and computationally,[6,7,10] and our model follows the mechanism from these reports. Our computationally optimized structures and reaction energies for the species presented in Scheme 3 are provided in Figure 1 and Table 1, respectively.

The insertion step is initiated by the coordination of the carbodiimide to the lithium center through a nitrogen lone

(24) (a) Kottmair-Maieron, D.; Lechler, R.; Weidlein, J. *Z. Anorg. Allg. Chem.* **1991**, *593*, 111–23. (b) Coles, M. P.; Hitchcock, P. B. *Chem. Commun.* **2002**, (23), 2794–2795.

(25) (a) Hagadorn, J. R.; Arnold, J. *Inorg. Chem.* **1997**, *36* (2), 132–133. (b) Grundy, J.; Coles, M. P.; Hitchcock, P. B. *Dalton Transactions* **2003**, (12), 2573–2577. (c) Richter, J.; Feiling, J.; Schmidt, H.-G.; Noltemeyer, M.; Brueser, W.; Edelmann, F. T. *Z. Anorg. Allg. Chem.* **2004**, *630* (8−9), 1269–1275. (d) Hill, N. J.; Findlater, M.; Cowley, A. H. *Dalton Trans.* **2005**, *19*, 3229–3234. (e) Findlater, M.; Hill, N. J.; Cowley, A. H. *Polyhedron* **2006**, *25* (4), 983–988. (f) Otero, A.; Fernandez-Baeza, J.; Antinolo, A.; Tejeda, J.; Lara-Sanchez, A.; Sanchez-Barba, L. F.; Lopez-Solera, I.; Rodriguez, A. M. *Inorg. Chem.* **2007**, *46* (5), 1760–1770.

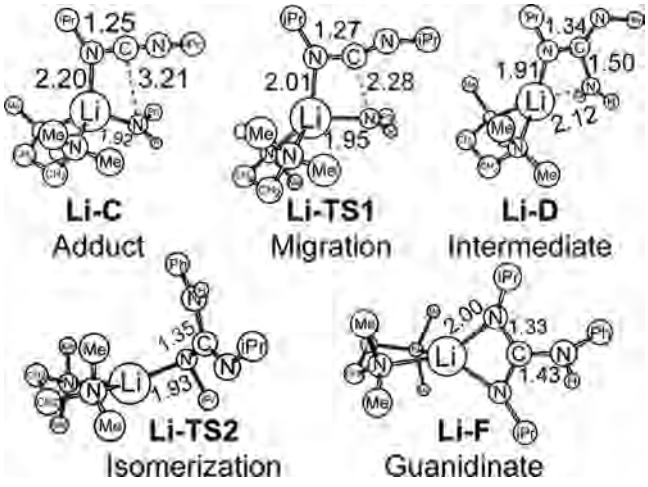

Figure 1. Optimized structures for the carbodiimide insertion step into the Li−NHPh bond. Labels correspond to Scheme 3 and Table 1.

pair of electrons, forming an adduct, **Li−C**. This coordination is relatively weak, with a Li−N(carbodiimide) bond distance of 2.20 Å. The energetic cost of dissociating the lithium dimer is only partially compensated for by the coordination energy of the carbodiimide, and as a result, the relative energy of the adduct, **Li−C**, is 14.6 kcal mol^{-1} higher than the free dimer, **Li−A**, and free carbodiimide.

Following the coordination of carbodiimide, the anilide group migrates to the central sp carbon of the carbodiimide, effecting an addition across a carbodiimide C−N double bond through the transition state, **Li−TS1**. The migration transition state is only 6.2 kcal mol^{-1} higher in free energy than the adduct, reflecting the highly polarized character of the Li−N bond undergoing insertion. Although the barrier for the migration is small with respect to the adduct, the migration transition state sits 20.8 kcal mol^{-1} relative to the free reactants. This addition leads to an intermediate species possessing a guanidinate isomer (**Li−D** in Scheme 3 and Figure 1), in which only one of the nitrogen centers originating from the carbodiimide is bonded to lithium. This ligand serves as an amido ligand (R_{Li-N} = 1.91 Å) with pendant electron lone pair donation from a phenylamine group (R_{Li-N} = 2.12 Å). The addition step is energetically favorable relative to the adduct formation (Table 1) due to the creation of a new C−N bond.

The remaining step of the insertion is an isomerization of the intermediate to form the appropriate guanidinate. This process is thermodynamically driven, with the guanidinate complex (**Li−F**) being 8.3 kcal/mol more stable than the intermediate, **Li−D**, due to the formation of the delocalized π system in the former. The isomerization can occur though a simple rotation around the Li−N−C−N dihedral, allowing the second sp^2 nitrogen to coordinate to the lithium metal and releasing the coordinated electron pair of the pendant group. The optimized transition state, **Li−TS2**, for this isomerization is depicted in Figure 1. During the isomerization process, the interaction between the migrated anilide group and the metal is lost, but because the interaction is not strong, the barrier for isomerization is modest (14.5 kcal mol^{-1}) and not rate-limiting.

When free guanidines (the product) are present in solution, there is an alternative reaction pathway that we have explored that avoids the isomerization transition state. This pathway is shown in the lower part of Scheme 3 where the intermediate **Li−D** coordinates with an additional guanidine molecule via its lithium center to form complex **Li−E**. The optimized structure of **Li−E**, shown in Figure 2, reveals that this complex possesses a hydrogen-bonding interaction between the N−H bond of the incoming guanidine and the coordinated nitrogen center of the existing guanidinate ligand. An XRD structure of a similar compound has been reported by Coles and Hitchcock,[26] wherein a neutral guanidine serves as a hydrogen-bond donor to a coordinated guanidinate. This interaction facilitates the transfer of the proton to the guanidinate ligand, which leads to the release of guanidine and formation of the complex **Li−F**. It should be emphasized that this process does not result in the net formation of a guanidine product, but it can be described as a near degenerate exchange of guanidine that has the same result as the direct isomerization previously considered.

We find that this pathway is not thermodynamically favorable, as the coordination of the incoming guanidine to the metal in **Li−E** is weak, resulting in complex **Li−E** being 22.9 kcal mol^{-1} less stable than the reactants. We attribute the weak coordination of the incoming guanidine to the TMEDA ligand mitigating the Lewis acidity of the lithium center. Although the barrier to proton transfer is moderate relative to that of the guanidine−intermediate complex, **Li−E**, the overall free energy of activation is nonetheless high, at 22.6 kcal mol^{-1} (the transition state structure, **Li−TS3**, for this is shown in Figure 2). As a result, the activation energy for this alternative pathway is higher than for the unimolecular isomerization mechanism, indicating that this pathway probably is not important in this catalytic cycle.

Proton Transfer Stage. The final step of the catalytic cycle requires the amine substrate to transfer a proton to the newly formed metal−guanidinate complex, **Li−F**, and release of the guanidine product. This occurs through a transition state (**Li−TS4**, Figure 3) where an incoming aniline coordinates to the lithium center and one of the coordinating nitrogen centers of the guanidinate detaches from the metal and accepts a proton from the aniline. The activation energy for this step is modest, at 11.6 kcal mol^{-1}. The transition state occurs when the proton is roughly equidistant (1.3 Å) from the guanidinate nitrogen and the aniline nitrogen, indicating that the aniline N−H bond is effectively broken. This transition state leads to a complex, **Li−G**, where the newly formed guanidine product is coordinated to the Li center via the lone pair of the sp^2 hybridized nitrogen, as shown in Figure 3. A hydrogen-bonding interaction is also available between the N−H bond of the guanidine and the nascent anionic anilide ligand with a N−H distance of 1.73 Å, resulting in a complex with a relative energy of 8.1 kcal mol^{-1}. The complexation between the metal amide and the guanidine is weak, so the guanidine

(26) Coles, M. P.; Hitchcock, P. B. *Chem. Commun.* **2005**, (25), 3165–3167.

Table 1. Relative Energies for the Reaction Steps Corresponding to the Lithium Amido Catalyzed Guanylation of Aniline with Carbodiimide As Depicted in Scheme 3 and Figure 1[a]

reaction stage	species	description	relative gibbs free energy (kcal mol^{-1})
carbodiimide insertion	**Li−B**	monomer	11.1
	Li−C	adduct	14.6
	Li−TS1	migration TS	20.8
	Li−D	intermediate	8.8
	Li−TS2	isomerization TS	14.5
	Li−F	guanidinate	0.5
guanidine exchange	**Li−E**	guanidine-intermediate adduct	22.9
	Li−TS3	guanidine exchange proton transfer TS	28.5
amine to guanidinate proton transfer	**Li−TS4**	proton transfer TS	11.6
	Li−G	guanidine complex	8.1

[a] The energies for the insertion steps are calculated relative to the dimerized lithium complex (**Li−A**) and free carbodiimide.

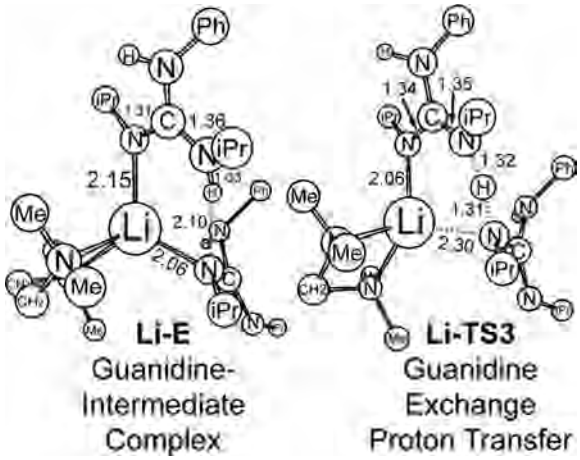

Figure 2. Guanidine−intermediate complex, **Li−E**, and guanidine proton transfer transition state, **Li−TS3**, for the alternative guanidinate formation mechanism.

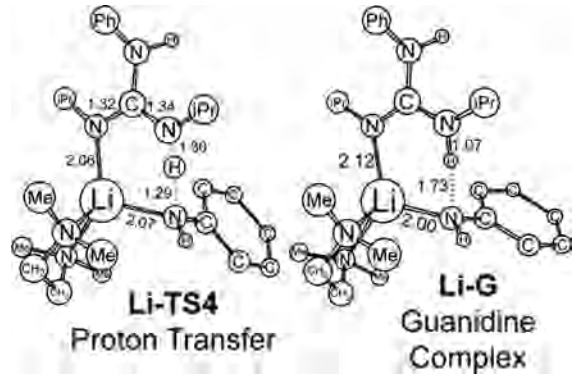

Figure 3. Proton transfer transition state structure (left) and the resulting guanidine product complex (right) for the proton transfer stage of the catalytic cycle.

product will readily dissociate from the metal to regenerate the monomeric catalyst, or alternatively, exchange can occur with an equivalent of carbodiimide to form the adduct **Li−C** as the first step in another catalyst turnover.

Aluminum Amides. Our computational results for the lithium amide catalyzed guanylation allow us to surmise that the essential features of this catalytic cycle require carbodiimide to insert into the metal−amide bond to form a guanidinate and a subsequent proton transfer from the amine to the guanidinate, releasing guanidine and regenerating the catalyst. From this and reactivity established in the literature, we thought that aluminum amides may also act as effective catalysts for the guanylation of amines. Carbodiimide is well-known to insert into aluminum amide bonds to form guanidinates in high yield.[4,6−9,24,27] Furthermore, Kenney et al. demonstrated that it is possible to insert a carbodiimide into an Al−NMe$_2$ bond of a diamido aluminum guanidinate at room temperature to form a bis(guanidinate) complex, indicating that aluminum guanidinates possess significant reactivity.[8] Moreover, in two reports by Hoerter et al., aluminum amides were found to be effective transamidation catalysts, which involves a similar proton transfer step.[21] The simplicity and economical nature, combined with the fact that they are relatively inert toward many common organic motifs, makes aluminum amides attractive as catalysts.

To evaluate whether aluminum amides could be efficient catalysts for the guanylation of amines, we calculated the intermediate and transition state structures for the guanylation of aniline with diisopropyl carbodiimide using an aluminum amide catalyst, following a catalytic cycle (Scheme 4) that is analogous to the cycle used for the lithium catalyzed guanylation. These calculations employed the aluminum amide Cl$_2$Al−NHPh as the putative active catalyst. The structure labeling is analogous to that found in the previous sections, except that the "Li" label is replaced with "Al".

Carbodiimide Insertion. The insertion of carbodiimide into group 13 amide bonds has been extensively studied both experimentally and computationally, and we have modeled this stage of the catalytic cycle within the established mechanism.[6,7,10] Optimized structures for the species in the catalytic cycle shown in Scheme 4 are presented in Figure 4 with the relative free energies given in Table 2. The insertion begins with the carbodiimide coordinating to the aluminum center to yield the adduct **Al−C**, which is only 1.6 kcal mol^{-1} less stable than the free carbodiimide and dimerized Al complex. An analogous B(III)−carbodiimide complex has been synthesized, consistent with our optimized structures.[10] This strong coordination contrasts with the Li system where the adduct **Li−C** is 14.6 kcal mol^{-1} less stable than the reactants. Migration of the amide ligand to the central sp carbon of the carbodiimide proceeds through the transition state structure (**Al−TS1**) and is facilitated by the lone pair of the amide, resulting in a modest barrier of 12.2 kcal mol^{-1} relative to the free reactants. This leads to the formation of

(27) (a) Grundy, J.; Coles, M. P.; Hitchcock, P. B. *J. Organomet. Chem.* **2002**, *662* (1−2), 178–187. (b) Cole, M. L.; Jones, C.; Junk, P. C.; Kloth, M.; Stasch, A. *Chem.−Eur. J.* **2005**, *11* (15), 4482–4491. (c) Brazeau, A. L.; Wang, Z.; Rowley, C. N.; Barry, S. T. *Inorg. Chem.* **2006**, *45* (5), 2276–2281.

Scheme 4. The Catalytic Cycle of the Guanylation of Aniline with Carbodiimide Using a Dichloro Aluminum Catalyst

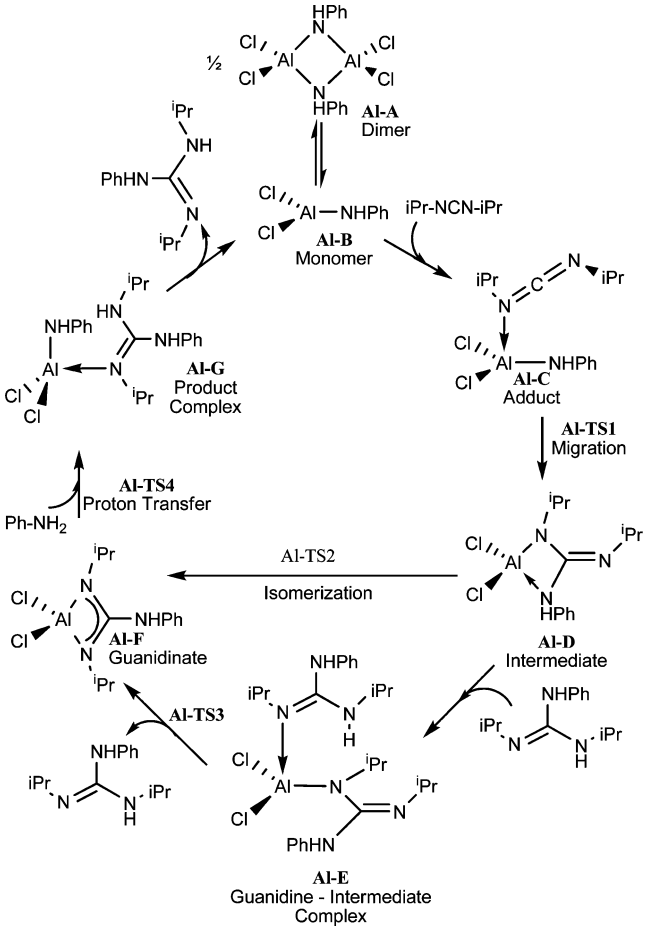

the intermediate, **Al−D**, in which the migrated amide group acts as a two-electron donor to the metal.

The formation of the guanidinate is the next step of the catalytic cycle and has been previously studied by quantum chemical calculations. Rowley et al.[7] evaluated the isomerization via rotation of the N(coordinated)−C(sp^2) bond, similar to what we presented in the previous section with the Li catalyst. The DFT calculations in that study predicted that this step is rate-limiting for carbodiimide insertion into aluminum amide bonds, as it requires complete cleavage of the metal-coordinated amide group before the guanidinate begins to form. In this study, we have identified an alternative transition state for the chelation of the guanidinate ring, wherein a free carbodiimide from solution coordinates to the metal, stabilizing it during isomerization (Figure 4, **Al−TS2−cat**). The calculated barrier height for this isomerization is lowered from 30.9 kcal mol^{-1} in the noncatalyzed reaction to 21.1 kcal mol^{-1} with the additional carbodiimide coordinated. Although we have used carbodiimide as the external base here, other potential ligands that are present in solution, such as the substrate or the guanidine product, could also act as the Lewis base in this step.

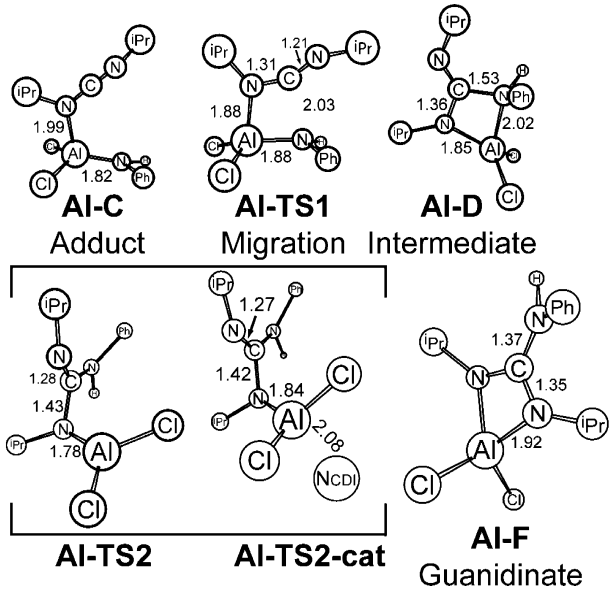

Figure 4. Reaction intermediates and transition states for the insertion of carbodiimide into the Al−NHPh bond. **Al−TS2−cat** is the isomerization transition state facilitated by the coordination of carbodiimide, where N_{CDI} refers to a nitrogen atom of a second carbodiimide which is acting as a catalyst.

Similar to our approach with the lithium catalysts, we have investigated an alternative to the isomerization, wherein a product guanidine present in solution coordinates to the insertion intermediate as shown in the lower part of Scheme 4. The calculated complex **Al−E** and transition state **Al−TS3** involved in this alternative mechanism are presented in Figure 5. As in the lithium amide catalyzed cycle, the incoming guanidine forms a metal-bound guanidinate in a near degenerate exchange. This step does not result in the net formation of the guanidine product; however, this mechanism does avoid **Al−TS2**, which is rate-limiting in this system. This alternative mechanism begins with the coordination of the guanidine to the intermediate, which is exergonic by 1.2 kcal mol^{-1}. The guanidine coordinates to the aluminum center through its imine lone pair and also forms a hydrogen bond through the guanidine's amine group and the nitrogen of the Al-bonded monodentate guanidinate. Proton transfer from the incoming guanidine to the aluminum-bound nitrogen is facile, with a free energy of activation of only 7.5 kcal mol^{-1}, enabling a guanidinate to form without the prohibitively high barrier of the unimolecular isomerization. The reason that this alternative mechanism is active for the Al catalyst but not for the Li catalyst is that the coordination of the additional guanidine to the Al center is much stronger than in the case of Li. Thermodynamically, the coordination of guanidine to form **Li−E** is endergonic, and the relative energy of the resultant complex lies at 22.9 kcal mol^{-1}, while the aluminum analogue (**Al−E**) is much more stable, with a relative energy of 4.7 kcal mol^{-1}.

Proton Transfer. The final step in the formation of guanidine product involves the proton transfer from the amine to guanidinate ligand in **Al−F**. The structural details of this transformation are presented in Figure 6. The transfer of hydrogen to the guanidinate occurs through a transition state where one of the coordinated nitrogen atoms of the guanidinate detaches from the metal and accepts a proton from the incoming amine. This is analogous to our observations on the lithium amide catalyzed transformation. At the transition state, the tetrahedral aluminum center displays two

Table 2. Relative Energies for the Reaction Steps for the Catalytic Cycle Scheme 4 and Figure 4[a]

reaction stage	species	description	relative gibbs free energy (kcal mol^{-1})
carbodiimide insertion	**Al−B**	monomer	17.4
	Al−C	adduct	1.6
	Al−TS1	migration	12.2
	Al−D	intermediate	5.2
	Al−TS2	isomerization TS (unimolecular)	30.9
	Al−TS2−cat	isomerization TS (Lewis base catalyzed)	21.1
	Al−F	guanidinate	−9.1
guanidine exchange	**Al−E**	guanidine-intermediate adduct	4.7
	Al−TS3	guanidine exchange proton transfer	16.6
amine to guanidinate proton transfer	**Al−TS4**	proton transfer	7.3
	Al−G	guanidine complex	−7.5

[a] The energies for the insertion steps are calculated relative to the dimerized aluminum complex and free carbodiimide, while the energies of the proton transfer steps are calculated relative to the aluminum guanidinate and aniline.

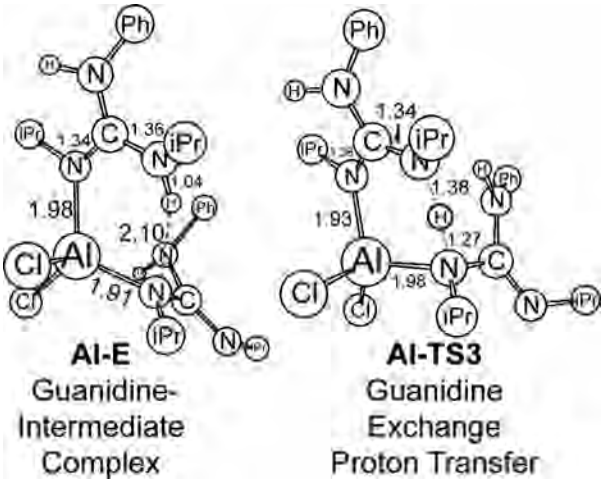

Figure 5. Optimized structures of the guanidine-intermediate complex, **Al−E**, and guanidine proton transfer transition state, **Al−TS3**, for the alternative guanidinate formation mechanism.

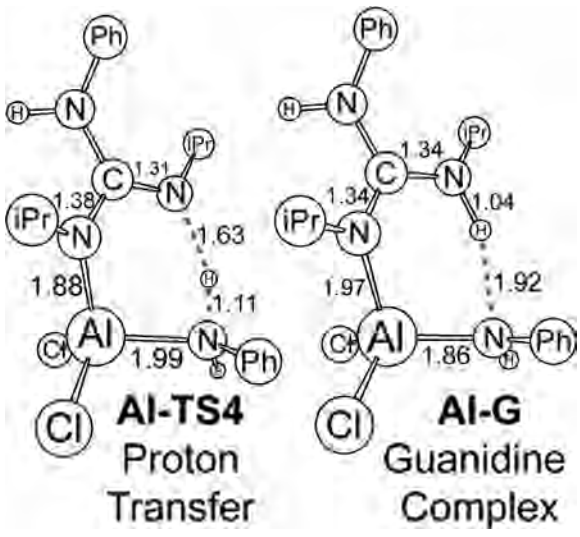

Figure 6. Transition state and product complex for the transfer hydrogenation of aluminum dichloro guanidinate by aniline. Selected bond lengths are reported in ångstroms.

nearly equivalent Al−N bonds (1.91 Å for the Al−N(guanidinate) bond vs 1.93 Å for the Al−N(amide) bond). As reported in Table 2, the barrier to this transfer is modest (16.5 kcal mol^{-1}), and somewhat higher than the barrier for the analogous step for the lithium guanidinate. Further, for the lithium guanidinate, the transition state occurs late in the reaction coordinate, with a N(aniline)−H bond length of 1.30 Å. The aluminum guanidinate transition state occurs much earlier, with a N(aniline)−H bond length of 1.11 Å. This trend can be interpreted through Hammond's postulate by considering the relative strengths of the bonds broken and formed in this step. While the N(aniline)−H and N(guanidine)−H bonds formed in this reaction are roughly equal in strength in each reaction, the metal−amide bond strengths are considerably different. The lithium−amide bond is largely ionic and relatively weak, and the creation of this bond does not strongly stabilize the late portion of the reaction coordinate, resulting in a late transition state. Conversely, the aluminum amide bond formed in this step is largely covalent and quite strong,[28] stabilizing the late portion of the reaction coordinate and resulting in an early transition state.

This transition state leads to a complex, **Al−G**, where the newly formed neutral guanidine is bound to the aluminum center via the lone pair of electrons of the sp^2 hybridized nitrogen. A hydrogen-bonding interaction is formed between the N−H bond and the lone pair of the newly formed amide ligand. Finally, dissociation of the guanidine from the aluminum center releases the product and regenerates the active catalyst.

Experimental Evaluation of the Al−Amido Catalyzed Guanylation. Although there are some notable differences in the computed pathway and energetic features for the guanylation of arylamines with carbodiimides between lithium amido species and aluminum amido compounds, our computational results suggest that Al−N(amido) groups should be proficient catalysts in this transformation. Thus, we initiated an experimental evaluation of Al−amido complexes as catalysts for the guanylation of electron-deficient aryl amines with carbodiimide, which are generally challenging substrates.

We began by testing some simple aluminum amido complexes as catalysts in this reaction. As a benchmark, we examined the room temperature guanylation of aniline with di(isopropyl)carbodiimide with a 5 mol % Al loading. Three catalyst precursors were employed in this initial screen: $Al(NMe_2)_3$, $AlClMe_2$, and $AlCl_3$. In all three cases, we anticipated that reaction with amine under the catalyst conditions would generate the required Al−anilido species. The results for this guanylation are summarized in Table 3

(28) Kormos, B. L.; Cramer, C. J. *Inorg. Chem.* **2003**, *42* (21), 6691–6700.

Table 3. Room Temperature Guanylation of Aromatic Amines Using Different Aluminum Precatalysts According to the Following Reaction Scheme

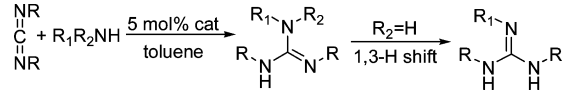

amine	carbodiimide	catalyst precursor	yield (%)[a]
$C_6H_5NH_2$	^{i}PrNCN^{i}Pr	$Al(NMe_2)_3$	64
		$AlClMe_2$	93
		$AlCl_3$	84

[a] All reactions were run for 18 h at room temperature

Table 4. Room Temperature Guanylation of Aromatic Amines with Carbodiimide Using 5 mol % $AlClMe_2$

entry	Ar′EH$_2$	RNCNR′	prod	yield (%)[a]
1	$C_6H_5NH_2$	^{i}PrNCN^{i}Pr	**1**	93
2	*p*-$H_2NC_6H_4NH_2$		**2**	100[b,d]
3	*p*-$H_2NCH_2C_6H_4NH_2$		**3**	78
4	*p*-$BrC_6H_4NH_2$		**4**	92[b]
5	2-$C_5H_4N(NH_2)$		**5**	78
6	$(C_6H_5)_2NH$		**6**	78[c]
7	$C_6H_5NH_2$	CyNCNCy	**7**	72
8	*p*-$H_2NC_6H_4NH_2$		**8**	98[b,d]
9	*p*-$H_2NCH_2C_6H_4NH_2$		**9**	93
10	*p*-$BrC_6H_4NH_2$		**10**	100[b]
11	2-$C_5H_4N(NH_2)$		**11**	100
12	$(C_6H_5)_2NH$		**12**	94[c]

[a] All reactions were run for 18 h. [b] Yield for reaction at 90 °C. [c] Yield for reaction at 70 °C. [d] Reaction was run for 2 days.

and show that $AlClMe_2$ demonstrated superior catalytic activity, producing guanidine in 93% yield. While the efficiency of this reaction depends on several extrinsic factors, such as catalyst stability and catalyst initialization, we can infer from the improved performance of $AlClMe_2$ over $Al(NMe_2)_3$ that the presence of electron-withdrawing chloride groups on the metal improves its activity.

We next employed the most efficient precursor, $AlClMe_2$, in a series of guanylation reactions with different amines and two different carbodiimides, as summarized in Table 4. These results clearly demonstrate the versatility of this catalyst for amine guanylations, and new guanidine compounds **5**, **9**, **10**, and **11** were synthesized with good yields. With some slight variation to reaction conditions, guanidine formation was achieved in yields varying from 72 to 100%.

Application of the aryl diamine, *p*-phenyldiamine, with two equivalents of carbodiimide (entries 2 and 8) demonstrated the ability of this system to react with both of the amine functions of the starting material. The product formed was a bisguanidine species $(RHN)_2C{=}N{-}(C_6H_4){-}N{=}C{-}(NHR)_2$, where R is either diisopropyl or cyclohexyl. This reaction did require slightly more forcing conditions (heating for 48 h) in order to achieve completion.

Aromatic C−Br bonds survived the catalytic conditions to yield the desired guanidine, as shown in entries 4 and 10. Analysis of these products by mass spectrometry provided a direct means to ensure the presence of the aryl bromide link in the product guanidine.

In some cases, slightly elevating the reaction temperature improved the guanidine yield. For example, when the reactions shown in entries 4 and 6 were carried out at 70 °C, the yield increased by about 10%. Some evidence of tolerance to potential coordinating functional groups is provided by the successful guanylation of 2-aminopyridine to yield products **5** and **11**. These species are new guanidine compounds that possess interesting pyridyl substituents.

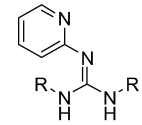

5 R = ^{i}Pr
11 R = Cy

Conclusion

A detailed catalytic cycle was elucidated, using DFT calculations, for the guanylation of aniline with carbodiimide, catalyzed by TMEDA−lithium complexes. The reaction mechanism proceeds through the coordination of carbodiimide to the lithium center, followed by the addition of the lithium−amido across the N=C bond of the carbodiimide. The reaction intermediate formed in this step isomerizes into a symmetric, bidentate guanidine. This process likely proceeds in a unimolecular step for this catalyst system. Finally, the guanidine is released through a proton transfer from the substrate amine, occurring through a transition state where one of the nitrogen centers of the chelating ligand detaches from the metal to abstract a proton from the substrate with concomitant bond formation between the lithium and the substrate. The activation energies for all of the steps in the catalytic cycle are modest, with all of them calculated to be less than 23 kcal mol^{-1}.

We extended this investigation to the analogous reactions of amines with carbodiimides using an amido(dichloro)aluminum catalyst, which we expected to show similar reactivity. A parallel reaction mechanism was identified for the aluminum catalyzed guanylation, albeit with two notable differences compared to the lithium catalyzed mechanism. First, the migration step of the carbodiimide insertion into the metal−amido bond has a significantly smaller barrier for the aluminum catalyst as compared to the lithium catalyst due to the high Lewis acidity of the three-coordinate aluminum center. Second, the barrier for the isomerization of the intermediate formed from the initial insertion is high for the aluminum catalysts. As a result, and in contrast to the lithium pathway, calculations suggest a bimolecular isomerization pathway involving the reaction of an existing guanidine with this intermediate as the most facile route to form the aluminum guanidinate. Despite the mechanistic differences compared to the Li catalyzed reaction, the activation energies for all steps of the catalytic cycle are also calculated to be modest for the Al catalyzed guanylation. Therefore, the calculations suggested that aluminum amides would also be effective amine guanylation catalysts.

We have confirmed through experiments that aluminum amides catalyze the guanylation of amines, and we found that a range of simple aluminum complexes are effective catalysts for the guanylation of anilines and aryl amines with carbodiimide in high yields. Using a variety of electron-deficient aryl amines, two different carbodiimides, and $AlClMe_2$ as the precatalyst, guanidine formation was achieved in yields varying from 72 to 100%, with some slight variation

to reaction conditions.

Given that yttrium, lithium, titanium, and now aluminum complexes have been found to efficiently catalyze the guanylation of amines through an insertion−proton-transfer mechanism, it is likely that a wide range of metals may be used. This study has allowed us to develop a framework for the further development and extension of these catalysts. The key requirements are that carbodiimide can insert into the metal amide to form a guanidinate ligand, and that a chelating nitrogen of the guanidinate can detach from the metal to accept the proton from the incoming amine. Metal amides that can readily form a guanidinate by carbodiimide insertion and also have flexibility in their coordination mode are prime candidates for this type of activity. Another direction to advance this chemistry, which we are currently exploring in our laboratories, involves the Li and Al catalyzed guanylation of phosphines and ethynes to form phosphaguanidines and propiolamidines, respectively. Finally, since a similar reaction mechanism has been outlined for aluminum amide catalyzed transamidation,[21] and since CN insertion into Al−NMe_2 bonds has recently been used to catalyze the cyclotrimerization of cynamide,[20] aluminum amides may have further utility as catalysts for other CN bond transformations.

Experimental Section

General Considerations. All manipulations were carried out in either a nitrogen-filled glovebox or under nitrogen using Schlenk-line techniques. Diisopropylcarbodiimide, dicyclohexylcarbodiimide, aniline, 4-aminobenzylamine, 4-bromoaniline, 2-aminopyridine, diphenylamine, *p*-phenyldiamine, and 1.0 M dimethylaluminumchloride in hexanes were purchased from Aldrich Chemical Co. and used without further purifications. Toluene, hexane, and ether were purified by passage through a column of activated alumina using an apparatus purchased from Anhydrous Engineering. ^1H and ^{13}C NMR were collected on a Bruker AVANCE 300 or 400 MHz spectrometer using the residual protons of the deuterated solvent for reference where applicable.

Preparation of N-Phenyl-N′,N″-diisopropylguanidine (1) Using Different Al Catalyst Precursors. In a Schlenk flask, diisopropylcarbodiimide (0.4 g, 3.17 mmol) and aniline (0.295 g, 3.17 mmol) were mixed in toluene. To this mixture was added 5% (0.158 mmol) of the aluminum catalyst precursor ($Al(NMe_2)_3$, $AlClMe_2$, or $AlCl_3$), and the reaction mixture was stirred overnight at room temperature. The reaction mixture was filtered, and the volatiles were removed under a vacuum to yield a white solid, **1**. This compound has been reported previously. The yields of **1** obtained from each catalyst precursor were as follows: $Al(NMe_2)_3$, 0.44 g (64%); $AlClMe_2$, 0.65 g (93%); and $AlCl_3$, 0.59 g (84%).[16]

Preparation of (^{i}PrNH)$_2$C=N−(C$_6$H$_4$)−N=C(^{i}PrNH)$_2$ (2) with $AlClMe_2$ as a Catalyst. In a Schlenk flask, diisopropylcarbodiimide (0.4 g, 3.17mmol), *p*-$H_2NC_6H_4NH_2$ (0.17 g, 1.58mmol), and 5% $AlClMe_2$ (7.31 mg, 0.079 mmol) were mixed in toluene. The reaction was heated to 90 °C and allowed to stir for 48 h. During this time, a white precipitate formed. The reaction mixture was filtered, and the volatiles from the white precipitate were removed under a vacuum to yield 0.57 g (100%). Spectroscopic data on this compound are comparable with reported data.[14,29,30]

Preparations of N-*p*-Aminomethylphenyl-N′,N″-diisopropylguanidine (3), N-2-Aminopyridine-N′,N″-diisopropylguanidine (5), N-Phenyl-N′,N″-dicyclohexylguanadine (9), N-*p*-Aminomethylphenyl-N′,N″-dicyclohexylguanidine (11), and N-2-Aminopyridine-N′,N″-dicyclohexylguanidine (13) with $AlClMe_2$ as a Catalyst. Following the procedure described above for the synthesis of **1** and using the appropriate reagents, compounds **3**, **5**, **8**, **9**, **11**, and **13** were obtained in yields as reported in Table 4. Spectroscopic data on these species are comparable with previously reported data.

Preparations of N-*p*-Bromophenyl-N′,N″-diisopropylguanidine (4), N-Diphenyl-N′,N″-diisopropylguanidine (6), (CyNH)$_2$C=N−(C$_6$H$_4$)−N=C(CyNH)$_2$ (10), N-*p*-Bromophenyl-N′,N″-dicyclohexylguanidine (12), and N-Diphenyl-N′,N″-dicyclohexylguanidine (14) with $AlClMe_2$ as a Catalyst. Following the procedure described above for the synthesis of **2** and using the appropriate reagents, compounds **4**, **6**, **7**, **10**, **12**, and **14** were obtained in yields as reported in Table 4. Spectroscopic data on these species are comparable with previously reported data.[14,23,29]

Computational Methods. The calculations presented here were made with density functional theory,[31] as implemented in Turbomole 5.9[32] using the PBE functional[33] and the def2-TZVPP basis set.[34] Energies include a correction for Gibbs free energy through standard statistical mechanical relations, as well as a zero-point energy correction calculated within the harmonic approximation. We evaluated a COSMO continuum solvent correction for the lithium-catalyzed guanylation of aniline with the solvent toluene and found that there was no significant effect on the reaction energies or barrier heights. As such, we have not included a solvent correction in any of the calculations reported in this paper.

Acknowledgment. We thank NSERC of Canada and the Canada Research Chairs program for funding. CNR thanks NSERC for a PGS scholarship and HPCVL for research scholarships. We are also grateful to CFI, the Ontario Research Fund, IBM Canada, HPCVL and SharcNet for providing computing resources.

IC801028M

(29) (a) Thomas, E. W.; Nishizawa, E. E.; Zimmermann, D. C.; Williams, D. J. *J. Med. Chem.* **1989**, *32* (1), 228–236. (b) Zhang, W.-X.; Nishiura, M.; Hou, Z. *Chem. Commun.* **2006**, (36), 3812–3814.
(30) Maksic, Z. B.; Baric, D.; Kovacevic, B. *J. Chem. Soc., Perkin Trans. 2* **1999**, (5), 1011–1017.
(31) Ziegler, T.; Autschbach, J. *Chem. Rev.* **2005**, *105* (6), 2695–2722.
(32) Ahlrichs, R.; Baer, M.; Haeser, M.; Horn, H.; Koelmel, C. *Chem. Phys. Lett.* **1989**, *162* (3), 165–9.
(33) Perdew, J. P.; Burke, K.; Ernzerhof, M. *Phys. Rev. Lett.* **1996**, *77* (18), 3865–3868.
(34) Weigend, F.; Ahlrichs, R. *PCCP* **2005**, *7* (18), 3297–3305.